S.D. CAMPOS

Applied Mathematics Laboratory-CCTS/DFQM, Federal University of São Carlos
(Sorocaba, São Paulo CEP 18052780, Brazil; e-mail: sergiodc@ufscar.br)

CHIRAL SYMMETRY RESTORATION USING THE RUNNING COUPLING CONSTANT FROM THE LIGHT-FRONT APPROACH TO QCD

UDC 539

In this work, the distance between a quark-antiquark pair is analyzed through both the confinement potential and the hadronic total cross- section. Using the Helmholtz free energy, the entropy is calculated near the minimum of the total cross-section through the confinement potential. A fitting procedure for the proton-proton total cross- section is carried out, defining the fit parameters. Therefore, the only remaining free parameter in the model is the mass-scale κ used to define the running coupling constant of the light-front the approach to QCD. The mass scale controls the distance r between the quark-antiquark pair and, under some conditions, allows the appearance of free quarks even within the confinement regime of QCD.

K e y w o r d s: confinement potential, running coupling, chiral symmetry.

1. Introduction

Chiral symmetry restoration is one of the most interesting issues in the phase diagram of Quantum Chromodynamics (QCD). As is well known, there is the evidence of a phase transition from the confinement phase to a non-confinement one at the saturation scale. It was predicted, for example, by lattice simulations [1–4]. These results were supported by the Beam Energy Scan (BES) program [5, 6], which recently analyzed the experimental data from the relativistic heavy-ion collisions.

As a fundamental ingredient, the internal entropy of colliding hadrons should be taken into account to offer a complete view of the chiral symmetry restoration in QCD. However, the suitable definition of entropy is a hard task in any physical system. For example, the entropy can be related to one-quarter of the black hole event horizon area or Shannon's information disorder approach.

Moreover, the correct definition of entropy is a problem that permeates several issues as, for example, the study of the entropy production in rotating black holes [7], in the so-called Ekpyrotic universe [8], in Szekeres spacetimes [9], in quark-gluon plasma [10], in light clusters [11], and decoherence processes [12], among others.

Recently, a maximal entropy calculation was introduced assuming saturation effects due to the properties of the factorizable gluon density [13]. This result is close to that obtained previously by Kharzeev and Tuchin [14], whose achievement is due to the Unruh effect (analogous to the Hawking effect) applied to hadrons in the accelerated rest frame. They found the transition temperature $T_s \approx Q_s/2\pi$ at the spontaneous symmetry breaking, where Q_s is the transferred momentum in the gluon rest frame.

On the other hand, a possible topological phase transition in a hadron was proposed in Ref. [15], allowing the chiral symmetry breaking below the saturation scale with the transition temperature $T_c \approx \approx 0.001$ GeV, far below the Hagedorn temperature. Thus, above T_c but below the Hagedorn temperature [16, 17], the appearance of a free quark state is allowed, resulting in an effect quite similar to the emergence of a free vortex in the XY model. It should

be stressed that the chiral symmetry breaking was previously predicted by McLerran and Pisarski [18] and Glozman and Wagenbrunn [19], whose possible explanation was given by the presence of the quark matter, presented years ago in [18, 19]. In this scenario, the chiral symmetry is restored even in the presence of hadronic matter.

In the present work, I suppose that the hadronic total cross-section, $\sigma_{\rm tot}(s)$, can be divided into a finite number of non-interacting disjoint 2D cells, each one containing a quark-antiquark ($q\bar{q}$) pair ($u\bar{u}$ and $d\bar{d}$) separated by a distance $r(s)$, depending on the energy $\sqrt{s}$ measured in the center-of-mass system [15]. This approach is analogous to the so-called Berezinskii–Kosterlitz–Thouless (BKT) phase transition, which occurs without spontaneous symmetry breaking [20, 21]. In that planar model, at low temperatures, the presence of a non-trivial vortex configuration is suppressed due to the binding effect caused by the vortex-antivortex interaction. At high temperatures above some critical value, the binding effect can be neglected, and the non-trivial vortex state arises.

The main goal of the present work is to account for the physical consequences of the confinement potential inside the cell containing the $q\bar{q}$-pair considering a naive model with finite temperature and null quark chemical potential. Then, the free quark state is achieved, when the spatial separation, $r(s)$, between quark and antiquark is less than r_0, the confining scale. Using some constraints, we obtain an asymptotic bound to the rise of $r(s)$ as the collision energy grows. Moreover, using the running coupling from the light-front holographic QCD (see [22] and references therein), the non-confinement regime is attained below the saturation scale for $\kappa \approx 0.002$ GeV. The mass scale κ emerges in de Alfaro, Fubini, and Furlan's attempt to build a fully invariant conformal Lagrangian theory [23]. In the example of the original work, the mass scale provides the necessary infrared cut-off of the theory, and once determined, the scale furnishes the remaining unknown parameters. In the present context introduced here, κ is used as a free parameter representing the *effective* mass of the cell, being straightly connected with the distance $r(s)$ as shall be seen.

The paper is organized as follows. In Section 2, I introduce the relation for the entropy, total cross-section, and the distance between the quark and antiquark in the cell. In Section 3 under some conditions, the possible existence of a chiral symmetry restoration in the confinement phase of QCD will be shown. Final remarks are left for Section 4.

2. Total Cross- Section and Entropy

First of all, it should be stressed that, due to the Fitzgerald–Lorentz length contraction, the hadron contracts in the direction of its motion, although its visual appearance, which depends exclusively on its motion, is invariant in special relativity [24,25]. Then, it is reasonable to suppose that some physical properties observed in 2D planar objects may occur in the hadron [15]. Here, we maintain the analogy between the hadron in high-energy collisions and 2D planar objects, as done elsewhere [15]. Thus, we assume that the hadronic total cross-section can be divided into a finite number of disjoint cells containing a single $q\bar{q}$-pair, where its components interact with each other through a confinement potential. Then, the entropy is written as [15]

$$S(s) = \ln\left(\frac{\sigma_{\rm tot}(s)}{\pi r^2}\right), \tag{1}$$

where $r = r(s)$ is the radius of the cell containing the $q\bar{q}$-pair. The above assumption is based on the well-known behavior of 2D planar objects with vortex-antivortex pairs, where the presence of a BKT phase transition allows the arising of new degrees of freedom and the emergence of a free vortex state [20, 21].

Although the experimental access to $r(s)$ is forbidden at the present-day energies, the theoretical determination of some physical bounds is possible, in principle, by using high-energy theorems, as well as taking different approaches to the entropy $S(s)$ into account. Therefore, we can rewrite relation (1) as

$$r^2 = \frac{1}{\pi}\,\sigma_{\rm tot}(s) e^{-S(s)}. \tag{2}$$

A remarkable realization of axiomatic quantum field theory in the early 1960s is the Froissart–Martin bound. However, despite its beauty, the Froissart–Martin result is an asymptotic inequality: It does not give us a hint about the behavior of $\sigma_{\rm tot}(s)$ at intermediate energies or even the "correct" functional form of $\sigma_{\rm tot}(s)$ at high energies. That bound is usually written as

$$\sigma_{\rm tot}(s) \leq \frac{\pi}{m_\pi^2}\ln^2(s/s_0), \tag{3}$$

where m_π is the pion mass, and $\sqrt{s_0}$ is some initial energy (usually $\sqrt{s_0} = 1.0$ GeV). Of course, for $0 < e^{-S(s)}$, we can write the inequality

$$r^2 \leq \left[\frac{1}{m_\pi^2}\ln^2(s/s_0)\right] e^{-S(s)}, \tag{4}$$

which acts as the upper bound for r. We note, in addition, that the total cross-section is related to the imaginary part of the forward scattering amplitude through the well-known optical theorem

$$\sigma_{\rm tot}(s) = \frac{{\rm Im}\, F(s)}{s}, \tag{5}$$

where $F(s)$ is the forward scattering amplitude. Thus, one can also write

$$r^2 = \left[\frac{{\rm Im}\, F(s)}{s}\right] e^{-S(s)}. \tag{6}$$

The use of a specific parametrizations for $\sigma_{\rm tot}(s)$ can help us to understand the behavior of r depending on $\sqrt{s}$. In addition, some known results can also be used: For example, for small values of the transferred momentum $\sqrt{|t|}$ in the center-of-mass system, the scattering amplitude is given mainly by its absorptive part. Then, we can use the differential cross-section, for instance, for $\sqrt{|t|} < 0.1$ GeV, to infer effects introduced by t in Eq. (6).

On the other hand, considering the result given by Eq. (4), we can analyze the distance r according to $e^{-S(s)}$.

Firstly, consider the case where $S(s)$ is not a logarithmic function of its variable. Then, for the increasing entropy of the form $S(s) \sim s/s_0$ (for example), the distance r fastly decreases, leading to the presence of free quarks due to the chiral symmetry restoration. In contrast, for a system with decreasing entropy of the form $S(s) \sim s_0/s$, the distance r increases, as the collision energy grows.

Secondly, let us consider that $S(s)$ is a logarithmic function of its variable. Then, for a system with a slowing increasing entropy given by $S(s) \sim \ln(s/s_0)$, r tends to zero for sufficiently high energies. Of course, the decreasing entropy case is given by $S(s) \sim$ $\sim \ln(s_0/s)$, which implies the increase of r, as s grows. Both situations, where the entropy decreases, as the collision energy grows, although interesting, are not treated here.

It is worth to note that the definition of $S(s)$ only makes sense here, when considering the relative distance between the q and $\bar{q}$. Accordingly, $S(s)$ should explicitly depend upon r. Following the approach presented here, I introduce the distance r in $S(s)$ considering the confinement potential, as shall be seen.

3. Finite Temperature: Far Below the Saturation Scale

3.1. Confinement Potential and Running Coupling in the Confinement Phase of QCD

As a key point of the problem, the internal energy of the colliding hadrons cannot be inferred from the first principles of QCD or thermodynamics. Thus, the use of the potential energy may be a useful approach to obtain some insights into the physical processes, as carried out since the 1950s [26–29].

There are several confinement potentials in the literature (e.g., see [30–34]). For simplicity, only the Cornell confinement potential [32–34] is considered, which is in good agreement with the experimental data for the light and heavy meson spectrum [35–37]. That potential is usually written as

$$V(r) = -\frac{4}{3}\frac{\alpha_s(r)}{r} + \sigma r, \tag{7}$$

where $\alpha_s(r)$ is the Fourier sine transform of the running coupling constant $\alpha_s(Q)$, and $\sqrt{\sigma}$ is the string tension. For static-source $\sqrt{\sigma} = 0.46$ GeV [38] while the average estimation $\sqrt{\sigma} = 0.405$ GeV is obtained for a cold strongly interacting matter [39]. Without loss of generality, we adopt hereafter $\sqrt{\sigma} = 0.4$ GeV.

The running coupling constant of QCD is far from having a unified definition within the confinement regime. Although the perturbative sector of QCD has a well-posed definition, the same does not occur in the non-perturbative regime, where several approaches can be used. Two basic examples of definitions are the "analytical" running coupling obtained by Shirkov and Solovtsov with use of the spectral density from Källén–Lehmann relation [40] and the running coupling from the light-front approach to QCD [41].

In this work, I use the light-front holographic QCD approach to the running coupling [22, 42], whose choice is based on both its simplicity and good description of the available experimental data [22]. In the light-front holographic approach, the running

coupling is set for all values of Q as [22]

$$\alpha_s(Q) = e^{-Q^2/4\kappa^2}, \tag{8}$$

where κ is the mass scale (also called the mass parameter) determined from the soft-wall model [43,44], and defined for the hadron as

$$M^2 = 4\kappa^2(L + S/2 + n), \tag{9}$$

where M is the hadron mass, L, S, and n refer to the internal orbital angular momentum, internal spin, and radial quantum number, respectively. The soft-wall model is based on a quadratic dilaton field [44] that yields a harmonic confining potential whose strength is measured by κ. The consequence of such potential is the breaking of conformal invariance.

It is important to stress that κ has a value that depends on the meson Regge trajectories analyzed, and settles down, in general, in the interval $0.3 \lesssim \kappa \lesssim 0.8$ GeV [43]. Note, in addition, that the linear Regge trajectories given by (9) were obtained due to the quadratic dilaton field approach [44]. However, this model entangles the explicit and spontaneous breaking of chiral symmetries [45]. It is also worth to stress that the linearity of Regge trajectories is not true everywhere, being more evident for light baryons and mesons [46]. Thus, definition (9) may not hold everywhere.

Usually, a value of $\kappa \approx 0.5$ GeV is required to describe mesons and baryon masses, as well as the hypothesis of linear Regge trajectories [41, 47]. This value also satisfactorily describes the trajectories of the ρ and K^* mesons [43]. In contrast, from fitting procedures for the nucleon form factors in the Anti-de Sitter (AdS)/QCD soft-wall model, one has $\kappa \approx 0.40$ GeV [48]. Moreover, from the analysis of form factors, the values of κ are lower than those for Regge trajectories and mass spectrum [43]. For example, $\kappa = 0.261 \pm 0.002$ GeV assuming a constant current quark mass $m_q = 0.005$ GeV in a model inspired in the AdS/QCD correspondence [49].

As aforementioned, I suppose that the mass scale κ represents the *effective* mass of the $q\bar{q}$-pair in the cell and, then, assume $\kappa \ll 1$ GeV. That constraint will be clarified further.

Returning to the running coupling constant, to avoid the use of the mnemonic rule of Quantum Mechanics $Q \sim 1/r$, we should use the Fourier sine transform of Eq. (8) since, as noted by Shirkov, this rule may not be true everywhere [50]. Then, for a rigorous mathematical approach, the Fourier sine transform of Eq. (8) can be written as [51]

$$\alpha_s(r) = \int_0^\infty e^{-Q^2/4\kappa^2} \sin(Qr) dQ, \tag{10}$$

which can be solved in terms of the Dawson integral function defined as [52, 53]

$$D(x) = e^{-x^2} \int_0^x e^{-y^2} dy^2, \tag{11}$$

closely related to the error function $erf(x)$ by [53]

$$D(x) = -i\,\frac{\pi}{2}\, e^{-x^2} erf(ix). \tag{12}$$

The function defined by Eq. (11) can be approximated by the following series expansion depending on x is close to the origin ($x \ll 1$) [53, 54]

$$D(x) = \sum_{j=0}^{\infty} \frac{(-1)^j 2^j}{(2j+1)!!} x^{2j+1} = x - \frac{2}{3}x^3 + \frac{4}{15}x^5 - ..., \tag{13}$$

where $n!!$ is the double factorial defined as

$$n!! = \prod_{j=0}^{k} (n - 2j), \tag{14}$$

for $k = \lceil n/2 \rceil - 1$, where $\lceil x \rceil$ is the ceiling function (least integer greater than or equal to x). In contrast, for large x, the Dawson function given by Eq. (11) has an asymptotic behavior given by [54]

$$D(x) \approx \frac{1}{2x} + \frac{1}{2^2 x^3} + \frac{1 \times 3}{2^3 x^5} + \frac{1 \times 3 \times 5}{2^4 x^7} + \dots . \tag{15}$$

The main goal is to study a possible chiral symmetry restoration, implying a small value for $x = \kappa r$. For the sake of simplicity, let us suppose that $r \lesssim r_h$ fm, where r_h is the hadron radius. To achieve the confinement phase of QCD, we impose the constraint $\kappa \ll 1$ GeV, for which one has $\kappa r \ll 1$. As a result, we can use the series given by Eq. (13) to represent the running coupling in the r-space, and, in particular, $(\kappa r)^3 \ll 1$. As shall be seen, the ratio

r/r_0, for which $r/r_0 < 1$ indicates that the non-confinement regime is achieved, depends strongly on the choice of κ.

It is worth to note that the mass scale is also present in the Fourier sine transform, since $x = \kappa r$, which introduces the need for a careful analysis to obtain the correct representation of $\alpha_s(r)$ through the Dawson function. Observe that the presence of the mass scale results, after the Fourier sine transformation given by Eq. (10), in a dimensionful running coupling written as

$$\alpha_s(r) = 2\kappa\sqrt{\frac{2}{\pi}}D(\kappa r) =$$

$$= 2\kappa\sqrt{\frac{2}{\pi}}\left[\kappa r - \frac{2}{3}(\kappa r)^3 + \frac{4}{15}(\kappa r)^5 - ...\right]. \quad (16)$$

Then, it is necessary to change $\bar{\alpha}_s(r) \to \alpha_s(r)/\kappa$ in the above definition to restore the dimensionless feature of the running coupling.

Now, considering the stated before, we can replace $\bar{\alpha}_s(r)$ in the confinement potential given by Eq. (7)

$$V(r) = -\frac{4}{3}\frac{\bar{\alpha}_s(r)}{r} + \sigma r = -\frac{8}{3}\kappa\sqrt{\frac{2}{\pi}} \times$$

$$\times\left[1 - \frac{2}{3}(\kappa r)^2 + \frac{4}{15}(\kappa r)^4 - ...\right] + \sigma r. \quad (17)$$

Accounting for the above constraints on κ and r, we can retain the series expansion up to the second order, allowing us to write the confinement potential as

$$V(r) = -\frac{4}{3}\frac{\bar{\alpha}_s(r)}{r} + \sigma r \approx -\frac{8}{3}\kappa\sqrt{\frac{2}{\pi}}\left[1 - \frac{2}{3}(\kappa r)^2\right] + \sigma r. \quad (18)$$

The above result indicates a confinement potential with a finite negative range given by

$$V(0) = -\frac{8}{3}\kappa\sqrt{\frac{2}{\pi}}, \quad (19)$$

and exclusively dependent on the mass scale.

3.2. Entropy

For the region close to the minimum of the total cross-section, the volume of the hadron is nearly constant, implying that the entropy can be obtained by using the Helmholtz free energy [15]

$$S_{\rm H}(s) = \frac{1}{T_c}V(r), \quad (20)$$

where $r = r(s)$, and the transition temperature T_c depends on the potential approach used and $T_c \approx \approx 0.001$ GeV for the Cornell potential [15]. It is worth to point out that (20) should be used only close to the minimum of $\sigma_{\rm tot}(s)$, since the Helmholtz free energy does not necessarily vanish elsewhere.

Here, the main assumption is that the entropy given by Eq. (1) can be defined by the Helmholtz free energy near the minimum of $\sigma_{\rm tot}(s)$. Thus, we can write

$$S(s) = \gamma S_{\rm H}(s), \quad (21)$$

where γ is a real parameter. Justifying such a choice is quite difficult and is based on the fact that both definitions depend on r at the minimum of $\sigma_{\rm tot}(s)$. For the sake of simplicity, I assume $\gamma = 1$, as it acts only as a scale of the problem.

Using the potential given by Eq. (18) and the entropy in Eq. (20), we can introduce a cut-off in the series expansion of the exponential in Eq. (2) if $V(r)/T_c \ll 1$. This cut-off can be obtained for $\kappa \sim T_c \ll 1$ GeV. If satisfied, these constraints indicate unambiguously the emergence of free quarks, as shall be seen. Then, the following approximation for r can be written:

$$r^2 \approx \sigma_{\rm tot}(s) - \frac{\sigma_{\rm tot}(s)}{T_c}\left[-\frac{8}{3}\kappa\sqrt{\frac{2}{\pi}}\left(1 - \frac{2}{3}(\kappa r)^2\right) + \sigma r\right], \quad (22)$$

according to the constraints on κ, r, and confinement potential adopted. Of course, different approaches for $V(r)$ and $\alpha_s(r)$ will produce distinct expressions for r. Moreover, there are definitions for $V(r)$ that are independent of the running coupling (see, e.g., [30]).

3.3. Total Cross-Section

Now, it is necessary to introduce a functional form for the total cross-section. Within the intermediate energy range. We can use the following simple parametrization for the total cross-section [55]:

$$\sigma_{\rm tot}(s) = a_1(s/s_0)^{a_2} + a_3\ln^{\alpha_{\mathbb{P}}(0)}(s/s_0), \quad (23)$$

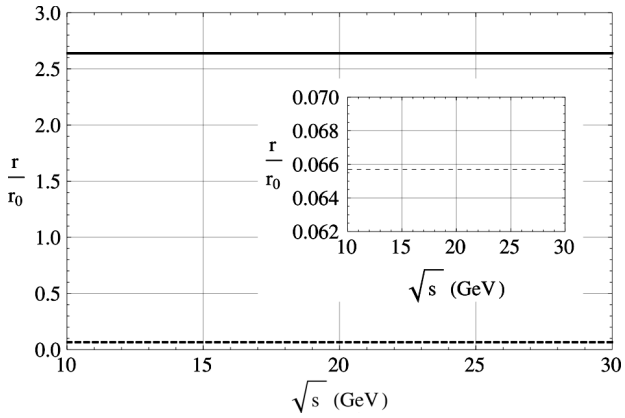

Fig. 1. Behavior of r/r_0 near the minimum of the total cross-section. Solid line is for $\kappa = 0.1$ GeV and dashed line is for $\kappa = 0.002$ GeV. Inner panel shows only the curve for $\kappa = 0.002$ GeV where $r/r_0 \approx 0.066$, indicating the presence of free quarks in the confinement phase of QCD

Parameters obtained using (23) in the fitting procedure assuming $\sqrt{s_0} = 1.0$ GeV ($\chi^2/ndf = 1.77$)

a_1 (mb)	a_2	a_3 (mb)	$\alpha_{\mathbb{P}}(0)$
52.52 ± 0.38	0.14 ± 0.01	0.91 ± 0.08	1.61 ± 0.03

where a_1, a_2, a_3, and $\alpha_{\mathbb{P}}(0)$ are free parameters. In the fitting process, we can use only the experimental data available for pp total cross-section above $\sqrt{s} = 3.0$ GeV (including cosmic-ray data) obtained from the Particle Data Group [56]. From the fitting procedure, we obtain the parameters shown in Table, where $\alpha_{\mathbb{P}}(0)$ is typical of the hard pomeron picture [57, 58].

As is well known, the hadronic total cross-section decreases, as the collision energy grows from some maximum located at $\sqrt{s} \approx 3.0$ GeV up to some minimum located in the energy interval $\sqrt{s} \approx 10 \sim$ ~ 30 GeV. This behavior is attributed to the odderon exchange, also known as the odd-C Regge exchange, a three-gluon state [59], recently observed [60]. This leading exchange differentiates particle-particle from particle-antiparticle scattering and, as $\sqrt{s}$ grows, this exchange becomes less important, implying that, at a sufficiently high energy, both total cross- sections tend to the same value (according to the Pomeranchuk theorem). In fact, this behavior for both $\sigma_{\rm tot}(s)$ at very high energies is attributed to the exchange of a particle called pomeron (not yet observed), which does not differentiate particle from antiparticle.

3.4. Results Depending on κ

Based on the above approaches and the result of the fitting, we have, as the only remaining free parameter, the mass scale κ.

Figure 1 shows the evolution of r/r_0 near the minimum of the total cross- section according to $\sqrt{s}$. As expected, it exhibits an almost flat behavior, as there is (almost) no variation on the hadronic total cross- section within this energy range. This result indicates that the distance between the $q\bar{q}$-pairs in the cell remains almost unchanged near the minimum of $\sigma_{\rm tot}(s)$. The solid line describes the evolution of r/r_0 for $\kappa = 0.1$ GeV (solid line) and for $\kappa = 0.002$ GeV (dashed line) in the energy range $\sqrt{s} = = 10 \sim 30$ GeV. For $\kappa = 0.1$ GeV, there is no emergence of a non-confinement phase, since $r/r_0 \approx 2.6$. In this situation, $r > 1$ fm may break the approximations performed here. In contrast, for $\kappa = 0.002$ GeV, the ratio $r/r_0 \approx 0.066$, indicating the unequivocal emergence of the chiral restoration in the confinement phase of QCD. It is worth to point out that $\kappa \sim m_q$, where m_q is the current quark mass (also $T_c \sim m_q/2$).

One observes that when κ diminishes, the distance r between the quark and the antiquark in the cell also decreases. Then, the mass scale measures the *effective* mass of the cell, and, when $\kappa \lesssim 0.002$ GeV, the quark and the antiquark are free to achieve new degrees of freedom. This does not mean that all pairs within the hadron will reach the non-confinement phase in this energy range: only the pairs, where $\kappa \lesssim 0.002$ GeV $\sim m_q$. The unbinding pairs are shielded by binding pairs that have not achieved the non-confinement phase, and, probably, these initial free quarks are created near the center of the hadron, explaining why we do not see these free states in the confinement regime of QCD.

It is important to stress that the chiral restoration can also be achieved assuming, for example, $\kappa \lesssim 0.035$ GeV, resulting in $r/r_0 \lesssim 0.94$. However, high values for κ cannot ensure the validity of the truncation of the exponential series performed to obtain Eq. (22).

The appearance of free quarks in the confinement phase of QCD at the center of the colliding hadron

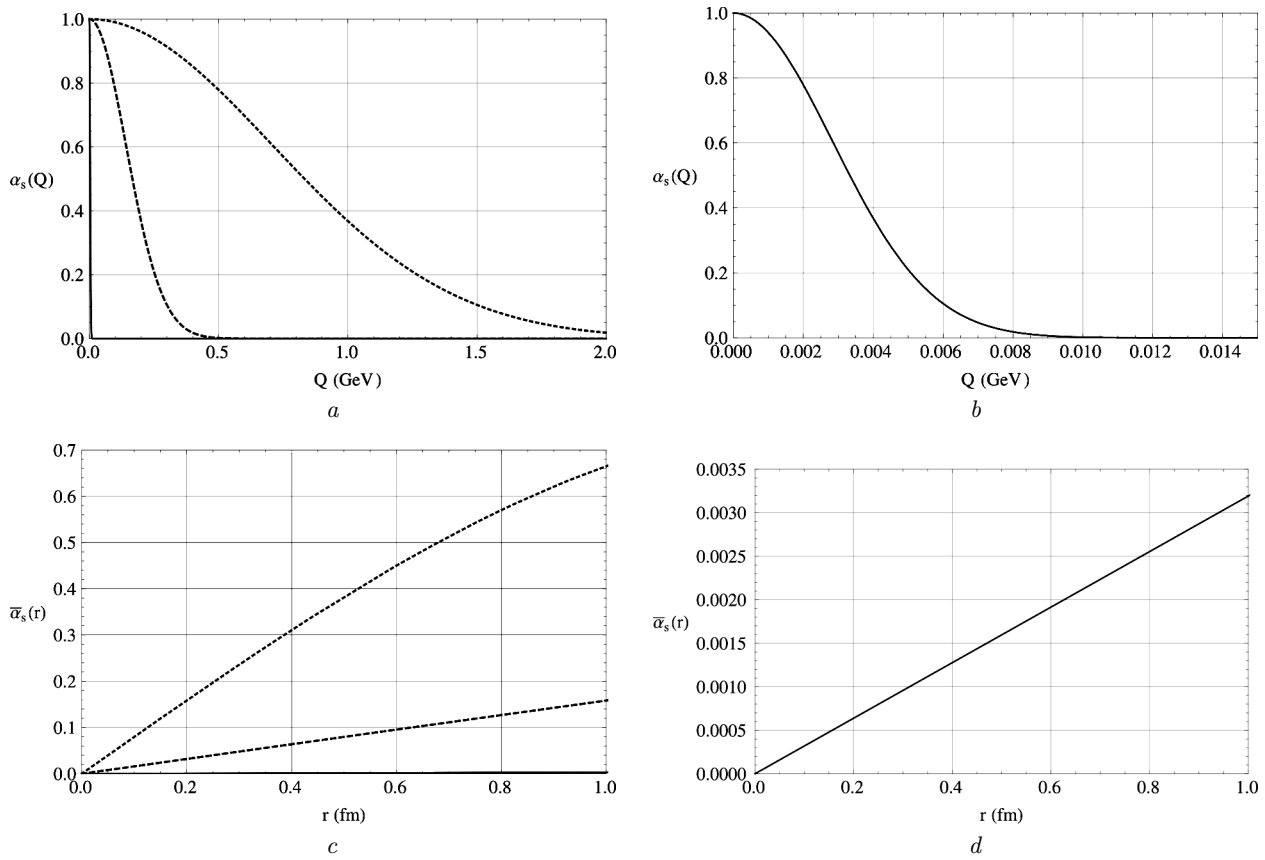

Fig. 2. For panels (a) and (c), solid line ($\kappa = 0.002$ GeV), dashed line ($\kappa = 0.1$ GeV), and dotted line ($\kappa = 0.500$ GeV). Panels (b) and (d) show the behavior of the running coupling for $\kappa = 0.002$ GeV. The fast decreasing of $\alpha_s(Q)$ in panel (b) represents a very slow increase in the position space (d)

may explain the hollowness effect [61, 62], marked by the appearance of a gray area near the center of the hadron (please, see [63], and references therein). This effect, broadly speaking, indicates that the black disk limit cannot be reached even for asymptotic energies.

In Fig. 2, panels (a) and (b) show the behavior of $\alpha_s(Q)$ using (8) and depending on κ. The solid line is for $\kappa = 0.002$ GeV (almost invisible in panel (a)), dashed line is for $\kappa = 0.1$ GeV, and for $\kappa = 0.500$ GeV we have the dotted line. Observe that the adoption of κ as a free parameter introduces the possibility of a non-confinement phase even for small Q. Panels (c) and (d) are for $\bar{\alpha}_s(r)$ using the same values for κ. In panel (c), the solid line for $\kappa = 0.002$ GeV is almost flat compared to the other curves, while, in panel (a), considering the same κ, the solid line presents a fast decrease.

4. Final Remarks

In the BKT phase transition, the vortex-antivortex pair is unbinding at the critical temperature. An analogy for this phase transition can be done by treating $q\bar{q}$-pairs like the vortex-antivortex pairs [15]. As obtained in this work, under certain physical conditions, the $q\bar{q}$-pairs can no longer exist even in the confinement phase of QCD. The possible restoration of the chiral symmetry in the confinement phase should be understood as the coexistence of free quarks and colorless states during the collision.

Interestingly, a few years ago was predicted both the existence of quark matter (which is not a quark) and the possibility that it suffers a chiral symmetry restoration in the confinement phase of QCD [18, 19]. According to McLerran and Pisarski [18], for a large number of colors N, it is reasonable that, for a large chemical potential μ_q and a low temperature,

a confining regime exists, as well as the preservation of the chiral symmetry.

Using the running coupling constant defined in the light-front approach to QCD, we obtain a confinement potential depending on the mass scale κ, considered here as the effective mass of the $q\bar{q}$-pair. The Helmholtz free energy close to the minimum of the total cross- section allows us to connect the entropy with the confinement potential. The fitting procedure is implemented to $\sigma_{\rm tot}(s)$ using pp experimental data. Then, the ratio r/r_0 is analyzed depending only on κ.

Considering the mass scale as a free parameter, it is assumed that κ represents the effective mass within the cell. For $\kappa = 0.002$ GeV, the ratio $r/r_0 \approx 0.066$ indicates the emergence of the chiral symmetry restoration in the confinement phase of QCD. It is important to stress that κ is close to the current quark mass, i.e., at the chiral symmetry restoration, one may expect $\kappa \sim m_q$. On the other hand, for $\kappa \gtrsim 0.035$ GeV, there is no emergence of free quarks in the confinement phase of QCD. In addition, we note that, in the 0.002 GeV$\lesssim \kappa \lesssim 0.035$ GeV interval, the chiral symmetry restoration is allowed, if the approximations performed could be ensured.

As a final conjecture, the decreasing of κ, resulting in the decreasing of r, may be a consequence of the odderon exchange occurring from some $\sqrt{s} \approx 3.0$ GeV up to the minimum of $\sigma_{\rm tot}(s)$. As the collision energy smoothly grows above the minimum of $\sigma_{\rm tot}(s)$, the odderon is no longer the leading particle exchange, which could imply a decrease in the emergence of free quarks. However, above the minimum of $\sigma_{\rm tot}(s)$, the creation of free quark through the odderon exchange, although less effective due to the diminishing (not the vanishing) in the odderon exchange, possibly continues up to the hadron dissociation (at the saturation scale). Since the emergence of free quarks leads to the increase of the entropy inside the hadron, then the growth of $\sigma_{\rm tot}(s)$ above the minimum may be caused (in thermodynamics language) by the increase of the entropy, which leads to the hadron dissociation at the saturation scale [64].

S.D.C. thanks the UFSCar for the financial support.

1. Y. Aoki *et al.* The QCD transition temperature: results with physical masses in the continuum limit II. *J. High. Energ. Phys.* **0906**, 088 (2009).
2. S. Borsanyi *et al.* (Wuppertal-Budapest Collaboration). Is there still any T_c mystery in lattice QCD? Results with physical masses in the continuum limit III. *J. High. Energ. Phys.* **1009**, 073 (2010).
3. C. Ratti. Lattice QCD and heavy ion collisions: a review of recent progress. *Rept. Prog. Phys.* **81**(8), 084301 (2018).
4. A. Bazavov *et al.* (USQCD Collaboration). Hot-dense lattice QCD: USQCD whitepaper 2018. *Eur. Phys. J. A* **55** (11), 194 (2019).
5. L. Adamczyk *et al.* (STAR Collaboration). Bulk properties of the medium produced in relativistic heavy-ion collisions from the beam energy scan program. *Phys. Rev. C* **96**(4), 044904 (2017).
6. A. Andronic *et al.* Decoding the phase structure of QCD via particle production at high energy. *Nature* **561** (7723), 321 (2018).
7. M. Cvetič, H. Lü, C.N. Pope. Entropy-product rules for charged rotating black holes. *Phys. Rev. D* **88**, 044046 (2013).
8. M. Li. Note on the production of scale-invariant entropy perturbation in the ekpyrotic universe. *Phys. Lett. B* **724**, 192 (2013).
9. L. Herrera *et al.* Vorticity and entropy production in tilted Szekeres spacetimes. *Phys. Rev. D* **86**, 044003 (2012).
10. S. Mattiello. Entropy production for an interacting quark-gluon plasma. *Nucl. Phys. A* **894**, 1 (2012).
11. Y.K. Vermani, R.K. Puri. Entropy and light cluster production in heavy-ion collisions at intermediate energies. *Nucl. Phys. A* **847**, 243 (2010).
12. R.J. Fries, B. Muller, A. Schäfer. Decoherence and entropy production in relativistic nuclear collisions. *Phys. Rev. C* **79**, 034904 (2009).
13. K. Kutak. Gluon saturation and entropy production in proton-proton collisions. *Phys. Lett. B* **705**, 217 (2011).
14. D. Kharzeev, K. Tuchin. From color glass condensate to quark-gluon plasma through the event horizon. *Nucl. Phys. A* **753**, 316 (2005).
15. S.D. Campos. Chiral symmetry in the confinement phase of QCD. *Mod. Phys. Lett. A* **36** (19), 2150135 (2021).
16. R. Hagedorn. Statistical thermodynamics of strong interactions at high energies. *Il Nuovo Cimento Suppl.* **3**, 147 (1965).
17. R. Hagedorn. Hadronic matter near the boiling point. *Il Nuovo Cimento A* **56**, 1027 (1968).
18. L. McLerran, R.D. Pisarski. Phases of dense quarks at large N_c. *Nucl. Phys. A* **796**, 83 (2007).
19. L.YA. Glozman, R.F. Wagenbrunn. Chirally symmetric but confined hadrons at finite density. *Mod. Phys. Lett. A* **23**, 2385 (2008).
20. V.L. Berezinskii. Destruction of long range order in one-dimensional and two-dimensional systems having a continuous symmetry group. I. Classical systems. *Zh. Eksp. Teor. Fiz.* **59**, 907 (1970); *Sov. Phys. JETP* **32**, 493 (1971).

21. J.M. Kosterlitz, D.J. Thouless. Ordering, metastability and phase transitions in two-dimensional systems. *J. Phys. C* **6**, 1181 (1973).
22. A. Deur, S.J. Brodsky, G.F. de Téramond. The QCD running coupling. *Prog. Part. Nuc. Phys.* **90**, 1 (2016).
23. V. de Alfaro, S. Fubini, G. Furlan. Conformal invariance in quantum mechanics. *Il Nuovo Cimento* **34** (4), 569 (1976).
24. J. Terrell. Invisibility of the Lorentz contraction. *Phys. Rev.* **116** (4), 1041 (1959).
25. R. Penrose. The apparent shape of a relativistically moving sphere. *Mathematical Proceedings of the Cambridge Philosophical Society* **55** (1), 137 (1959).
26. D. Bohm. A suggested interpretation of the quantum theory in terms of "hidden" variables. I. *Phys. Rev.* **85**, 166 (1952); ibid 180 (1952).
27. Sh. F.Y. Liu, R. Rapp. An in-medium heavy-quark potential from the $Q\bar{Q}$ free energy. ArXiv: 1501.07892[hep-ph].
28. G. Dennis *et al.* Fermi's ansatz and Bohm's quantum potential. *Phys. Lett. A* **378**, 2363 (2014).
29. G. Dennis, M.A. de Gosson, B.J. Hiley. Bohm's quantum potential as an internal energy. *Phys. Lett. A* **379**, 1224 (2015).
30. C. Quigg, J.L. Rosner. Quarkonium level spacings. *Phys. Lett. B* **71**, 153 (1977).
31. C. Quigg, J.L. Rosner. Quantum mechanics with applications to quarkonium. *Phys. Rep.* **56** (4), 167 (1979).
32. E. Eichten *et al.* Spectrum of charmed quark-antiquark bound states. *Phys. Rev. Lett.* **34**, 369 (1975).
33. E. Eichten *et al.* Charmonium: the model. *Phys. Rev. D* **17**, 3090 (1978).
34. E. Eichten *et al.* Charmonium: comparison with experiment. *Phys. Rev. D* **21**, 203 (1980).
35. M.G. Olsson, S. Vesell, K. Williams. Observations on the potential confinement of a light fermion. *Phys. Rev. D* **51**, 5079 (1995).
36. D. Ebert, V.O. Galkin, R.N. Faustov. Mass spectrum of orbitally and radially excited heavy-light mesons in the relativistic quark model. *Phys. Rev. D* **57**, 5663 (1998); Erratum *Phys. Rev. D* **59**, 019902 (1998).
37. E.J. Eichten, C. Quigg. Mesons with beauty and charm: spectroscopy. *Phys. Rev. D* **49**, 5845 (1994).
38. S. Aoki *et al.* $2+1$ flavor lattice QCD toward the physical point. *Phys. Rev. D* **79**, 034503 (2009).
39. A.P. Trawiński *et al.* Effective confining potentials for QCD. *Phys. Rev. D* **90**, 074017 (2014).
40. D.V. Shirkov, I.L. Solovtsov. Analytic model for the QCD running coupling with universal $\alpha_s(0)$ value. *Phys. Rev. Lett.* **79**, 1209 (1997).
41. S. J.Brodsky *et al.* Meson/baryon/tetraquark supersymmetry from superconformal algebra and light-front holography. *Int. J. Mod. Phys. A* **31** (19), 1630029 (2016).
42. S.J. Brodsky, G.F. de Téramond, A. Deur. Nonperturbative QCD coupling and its β function from light-front holography. *Phys. Rev. D* **81**, 096010 (2010).
43. S.J. Brodsky, H.G. Dosch, J. Erlich. Light-front holographic QCD and emerging confinement. *Phys. Rept.* **584**, 1 (2015).
44. A. Karch *et al.* Linear confinement and AdS/QCD. *Phys. Rev. D* **74**, 015005 (2006).
45. P. Zhang. Linear confinement for mesons and nucleons in AdS/QCD. *J. High. Energ. Phys.* **2010** (5), 39 (2010).
46. A.J.G. Hey, R.L. Kelly. Baryon spectroscopy. *Phys. Rep.* **96**, 71 (1983).
47. T. Branz *et al.* Light and heavy mesons in a soft-wall holographic approach. *Phys. Rev. D* **82**, 074022 (2010).
48. D. Chakrabarti, C. Mondal. Nucleon and flavor form factors in a light front quark model in AdS/QCD. *Eur. Phys. J. C* **73**, 2671 (2013).
49. A. Bacchetta, S. Cotogno, B. Pasquini. The transverse structure of the pion in momentum space inspired by the AdS/QCD correspondence. *Phys. Lett. B* **771**, 546 (2017).
50. D.V. Shirkov. Fourier transformation of the renormalization-invariant coupling. *Theor. Math. Phys.* **136** (1), 893 (2003).
51. A. Erdélyi *et al.* Tables of integral transforms (McGraw-Hill, 1954) [ISBN: 978-0070195509].
52. H.G. Dawson. On the numerical value of $\int_0^h ex^2dx$. *Proceedings of the London Mathematical Society*, **s1-29** (1), 519 (1897).
53. M. Abramowitz, I.A. Stegun. *Error function and Fresnel integrals. Handbook of mathematical functions with formulas, graphs, and mathematical tables* (9th ed. New York, 1972) [ISBN: 9780486612720].
54. F.G. Lether, P.R. Wenston. Elementary approximations for Dawson's integral. *Journal of Quantitative Spectroscopy and Radiative Transfer* **46** (4), 343 (1991).
55. S.D. Campos. Logarithmic Regge pole. *Chin. Phys. C* **44**, 103103 (2020).
56. M. Tanabashi *et al.* (Particle Data Group). Review of particle physics. *Phys. Rev. D* **98**, 030001 (2018).
57. E.A. Kuraev, L.N. Lipatov, V.S. Fadin. Multiregge processes in the Yang–Mills theory. *Sov. Phys. JETP* **44**, 443 (1976).
58. Y.Y. Balitsky, L.N. Lipatov. The Pomeranchuk singularity in quantum chromodynamics. *Sov. J. Nucl. Phys.* **28**, 822 (1978).
59. J. Bartels. High-energy behaviour in a non-abelian gauge theory (II). First corrections to $Tn \to m$ beyond the leading In s approximation. *Nucl. Phys. B* **175** (3), 365 (1980).
60. G. Antchev *et al.* (TOTEM Collaboration). First determination of the ρ parameter at $\sqrt{s} = 13$ TeV: probing the existence of a colourless C-odd three-gluon compound state. *Eur. Phys. J. C* **79**, 785 (2019).
61. I.M. Dremin. Interaction region of high energy protons. *Phys. Uspekhi* **58**, 61 (2015).
62. I.M. Dremin. Unexpected properties of interaction of high-energy protons. *Phys. Uspekhi* **60** (4), 333 (2017).
63. S.D. Campos, V.A. Okorokov, C.V. Moraes. The Tsallis entropy and the BKT-like phase transition in the impact

parameter space for pp and $\bar{p}p$ collisions. *Phys. Scr.* **95**, 025301 (2020).
64. S.D. Campos, A.M. Amarante. The effects of the Tsallis entropy in the proton internal pressure. *Int. J. Mod. Phys A* **35**, 2050095 (2020).

Received 11.02.22

С.Д. Кампос

ВІДНОВЛЕННЯ КІРАЛЬНОЇ СИМЕТРІЇ З ВИКОРИСТАННЯМ РУХОМОЇ КОНСТАНТИ ЗВ'ЯЗКУ В НАБЛИЖЕННІ СВІТЛОВОГО ФРОНТУ У КХД

Оцінюється відстань між частинками для пари кварк-антикварк з використанням потенціалу конфайнмента та повного перерізу розсіяння адронів. Базуючись на вільній енергії Гельмгольца, розраховано ентропію як функцію потенціалу конфайнмента біля мінімуму повного перерізу розсіяння. Виконано опис повного протон-протонного перерізу розсіяння, де єдиним вільним параметром моделі є масовий масштаб κ, що визначає константу зв'язку для світлового фронту в КХД. Масштаб мас контролює відстань r для пари кварк-антикварк і допускає при деяких умовах появу вільних кварків навіть у режимі КХД з конфайнментом.

Ключові слова: потенціал конфайнмента, рухома константа зв'язку, кіральна симетрія.